

*An automatic recognition system of
Brazilian flora species based on textural
features of macroscopic images of wood*

**Deivison Venicio Souza, Joielan Xipaia
Santos, Helena Cristina Vieira, Tawani
Lorena Naide, Silvana Nisgoski & Luiz
Eduardo S. Oliveira**

Wood Science and Technology

Journal of the International Academy of
Wood Science

ISSN 0043-7719

Wood Sci Technol

DOI 10.1007/s00226-020-01196-z



Your article is protected by copyright and all rights are held exclusively by Springer-Verlag GmbH Germany, part of Springer Nature. This e-offprint is for personal use only and shall not be self-archived in electronic repositories. If you wish to self-archive your article, please use the accepted manuscript version for posting on your own website. You may further deposit the accepted manuscript version in any repository, provided it is only made publicly available 12 months after official publication or later and provided acknowledgement is given to the original source of publication and a link is inserted to the published article on Springer's website. The link must be accompanied by the following text: "The final publication is available at link.springer.com".



An automatic recognition system of Brazilian flora species based on textural features of macroscopic images of wood

Deivison Venicio Souza¹ · Joielan Xipaia Santos² · Helena Cristina Vieira² · Tawani Lorena Naide² · Silvana Nisgoski² · Luiz Eduardo S. Oliveira³

Received: 12 January 2020
© Springer-Verlag GmbH Germany, part of Springer Nature 2020

Abstract

Advances in species recognition technologies can contribute to the conservation and protection of flora species, especially those threatened with extinction. The aim of this research was to compare the early fusion approaches of operators known as Local Binary Patterns (LBP) and late fusion, carried out at the level of the decision classifiers, in the construction of an automatic recognition system of forest species. 1901 macroscopic images of wood from 46 Brazilian species were used. The extraction of image characteristics was done using two variants of the LBP descriptor, covering different aspects of spatial and angular resolution. The repeated stratified k-fold cross-validation method was used to estimate the performance of the classifiers. The cross-validation folds were created using stratified random sampling, whose strata were the prediction classes. An automatic recognition system based on the concatenation of rotation-invariant LBP histograms and the SVM classifier showed an F1-score of 97.67%. The fusion of classifiers, through majority voting, improved the F1-score of this system by 0.33% point. This experiment revealed that more than 50% of the species showed no misclassification or occurred only once or twice. It was identified that some groups of species generally confused by wood anatomists were perfectly differentiated by this classification system. The recognition system showed good ability to identify species, and if this technology is combined with traditional identification tools and empirical knowledge, it is possible to minimize errors in the identification of Brazilian flora, especially endangered species, for which the proposed classification system showed high accuracy.

✉ Deivison Venicio Souza
deivisonvs@ufpa.br

¹ Faculty of Forestry Engineering, Federal University of Pará - UFPA, Coronel José Porfírio street, 2515, Altamira, Pará, Brazil

² Department of Forest Engineering and Technology, Federal University of Paraná - UFPR, Av. Prefeito Lothário Meissner - Jardim Botânico, Curitiba, PR, Brazil

³ Department of Informatics, Federal University of Paraná - UFPR, Coronel Francisco Heraclito dos Santos Street, 100, Jardim das Américas, Curitiba, PR, Brazil

Introduction

Brazil stands out in the world for its extensive native forest areas (IBÁ 2016), with a significant fraction of the global diversity of fungi and plants (between 9.5 and 9.9%), consisting of 18,932 endemic species, one of the highest rates of endemism (46.2%) on the planet (Forzza et al. 2010). However, Brazil's wide plant species biodiversity is threatened by habitat destruction and fragmentation, posing a serious risk of species extinctions (Costa et al. 2016). In the Brazilian Amazon, for example, Martinelli and Moraes (2013) estimated the existence of 87 endangered species, 90 with insufficient data and 142 not threatened, but considered of interest for conservation and research. The endangered species were fully included in Edict 443 from the Environmental Ministry (MMA) on December 17, 2014, which established the "Official National List of Endangered Flora Species", classified in the categories Extinct in the Wild (EW), Critically Endangered (CR), Endangered (EN), and Vulnerable (VU), all of which theoretically must be protected in their entirety, including the prohibition of collection, harvesting, extraction, transportation, storage, processing, and marketing, among others (MMA 2014).

The correct identification of species is one of the fundamental aspects for the conservation of flora. In the scientific community, traditional mechanisms for identifying forest species include botanical or dendrological characterization and/or analysis of macroscopic and microscopic anatomical structures (Muñiz et al. 2016; Bila et al. 2018; Soffiatti et al. 2016). The recognition process is commonly guided by identification keys, such as that provided by the International Association of Wood Anatomists (IAWA) (Wheeler et al. 1989). Although very effective, these identification mechanisms require a high level of qualification in terms of theoretical knowledge and practical experience. In the practical activities of forest inventories (FI), this professional category exists, called "parabotanist", but, unfortunately, these specialists are increasingly rare. In addition, in the Amazonian context, identification activities in FI do not rely on the expertise of a parabotanist, but rather on the empirical knowledge of natives, who have gained practical experience over generations and use vernacular names in the identification process. The use of these names is problematic, since it groups distinct species, creating risk of species extinction, incorrect use of wood, and, consequently, incredulity in the seller–consumer relationship (Procópio and Secco 2008).

In this context, studies aimed at the correct identification of flora species are crucial for the conservation and protection of biodiversity. Fortunately, current researchers have awakened the potential of modern approaches, such as machine learning and computer vision, to recognize plant species (Martins et al. 2013; Paula Filho et al. 2014; Maruyama et al. 2018; Yigit et al. 2019). Advances in species recognition technologies are important, and if combined with the traditional identification tools and empirical knowledge, they can be an effective strategy to reduce field errors in identifying species of Brazilian flora.

Studies involving computer vision commonly focus on the use of leaf and wood images (macroscopic and microscopic) for feature extraction and development of automatic classifiers. A study reported in Yigit et al. (2019) used leaf visual

characteristics to construct an automatic identifier to recognize 32 plant species, achieving accuracy of 92.91% when using the Support Vector Machine (SVM) algorithm. In Martins et al. (2013), 2240 microscopic images of 112 forest species were employed, and the combined use of the feature extractor known as the Local Binary Pattern along with the SVM classifier ensured a better performance (98.6% and 86.0%) for both experiments. The study of Martins et al. (2015) used the same microscopic imaging base as Martins et al. (2013) and found 93.03% recognition rate using a dynamic sorter selection method. Species-recognition research based on native wood charcoal images using the descriptor called Local Binary Patterns (LBP) associated with machine learning classifiers and convolutional neural networks achieved recognition rates over 90% (Maruyama et al. 2018). Paula Filho et al. (2014) proposed a divide and conquer strategy and achieved a 9% improvement in the recognition rate using macroscopic images of wood, and the best accuracy was 97.77%. It is noteworthy that the use of digital images has other potential advantages, as reported by Kuo and Wang (2019), who obtained promising results in the prediction of elastic properties of juvenile and adult *Cryptomeria japonica* wood. In addition, it is possible to use other forms of wood classification. Deklerck et al. (2019) proposed a protocol for automated identification using the metabolome profile (acquired with direct analysis in real-time mass spectrometry) and obtained good results for the differentiation of wood of Meliaceae species.

For the description of texture based on images, the LBP method has attracted a good deal of attention by the scientific community (Liu et al. 2017), especially after the introduction in 2002 of the operators $LBP_{P,R}^{u2}$ (uniform LBP) and $LBP_{P,R}^{riu2}$ (uniform and rotation-invariant LBP) by Ojala, Pietikäinen, and Mäenpää (Ojala et al. 2002). Therefore, the purpose of this paper is to compare LBP feature aggregation strategies, extracted under different realizations of their parameters (P and R), and also the fusion of classifiers using the majority vote as a final decision rule, aiming to build an accurate automatic forest species recognition system based on macroscopic images of wood from Brazilian native and exotic species.

Wood database

Wood samples were from the collection of the Wood Anatomy and Quality Laboratory (LANAQM) of Federal University of Paraná (UFPR), located in Curitiba, Paraná. The wood samples' transversal surfaces were sanded with a 120 sandpaper and macroscopic images of 46 species were taken with a Zeiss Discovery V 12 stereomicroscope, with size of 2080×1540 pixels and $10\times$ magnification. The captured images have a resolution of 150 dpi. A total of 1,901 macroscopic images were obtained. Compared to the study by Paula Filho et al. (2014), this base includes new commercially confused species, even in replacement of some endangered Brazilian species. Furthermore, instead of using a stereomicroscope to capture images as done here, Paula Filho et al. (2014) applied an acquisition protocol to a box with two halogen lamps located on the sides while the wood sample was positioned at the

bottom, and took images using a Sony DSC T20 camera with the macro function activated.

Of the 46 species used in this study, 7 (15%) are on Brazil's official list of endangered species. More specifically, the species *Araucaria angustifolia* and *Ocotea porosa* are classified in the category "Endangered", *Cedrela fissilis*, *Bertholletia excelsa*, *Mezilaurus itauba*, and *Swietenia macrophylla* are part of the "Vulnerable" group, and *Euxylophora paraensis* is considered "Critically Endangered". Table 1 lists the 46 species of Brazilian trees (native and exotic) considered in the present study. The number of samples was variable in each species. Two images were obtained by samples, i.e., one in each transversal surface. However, some images were discarded due to defects, such as very large grooves. Figure 1 presents macroscopic images of some wood samples. The data described in this study are available at Mendeley Data (DOI: 10.17632/cc78ftcdf9.1).

The scientific names of the species in Table 1 are hyperlinks to **Brazilian Flora 2020** and **Tropicos** (Missouri Botanical Garden) web pages. In the hyperlinks, a detailed description of the species, as well as geographic distribution, phytogeographic domains, vegetation type of occurrence, among others, is found.

Local binary patterns: review

The process of extracting image characteristics is critical to the success of the automatic classifier modeling step. Good discriminative data increase the chance of building smart recognition systems with good ability to identify reality. This section provides a brief description of the method known as Local Binary Patterns (LBP), a successful texture descriptor widely used in computer vision.

The manuscript published by He and Wang (1990) was a milestone, because it described a new statistical method for texture analysis of images called texture spectrum, based on the concept of texture unit (TU). TU was defined as the smallest complete unit that best characterizes the local texture spectrum of a given pixel and its neighborhood in all eight directions of a square scan. From this, the texture of an image is characterized by its texture spectrum, which describes the distribution of all TUs within the image. Thus, a TU can be represented by eight elements situated in a square neighborhood of 3×3 pixels, where each element can assume three possible values (0, 1 or 2). Therefore, from the combination of the eight elements, it is possible to extract $3^8 = 6561$ patterns of local textures (He and Wang 1990).

Ojala et al. (1994) proposed a two-level adapted version of the approach proposed by He and Wang, providing a robust way to describe local binary patterns (LBP) of image texture, being invariant in grayscale. In the two-level version (0, 1), the number of possible texture units has been reduced to $2^8 = 256$. The LBP operator calculation steps can be simplified as follows: (1) neighborhood: establish a 3×3 neighborhood around a center pixel; (2) thresholding: threshold the grayscale values of the eight neighbors by comparing them with the intensity of the central pixel, and when the central pixel value is greater than or equal to the value of its neighbor, assign "1", otherwise "0", resulting in an eight-digit binary number (10001011); (3) weights: multiply each binary code (Fig. 2b) by a weight, observing its position in

Table 1 Family, scientific name, number of samples, number of macroscopic images by species, and classification of endangered species in the official list of Brazil

Code	Family	Scientific Name	Samples	N	Category ^a
1	Fabaceae	<i>Acrocarpus fraxinifolius</i> Arn.	9	17	
2	Araucariaceae	<i>Araucaria angustifolia</i> (Bertol.) Kuntze	28	55	EN
3	Apocynaceae	<i>Aspidosperma polyneuron</i> Müll. Arg.	10	20	
4	Apocynaceae	<i>Aspidosperma</i> Mart. & Zucc.	21	41	
5	Moraceae	<i>Bagassa guianensis</i> Aubl.	26	52	
6	Rutaceae	<i>Balfourodendron riedelianum</i> (Engl.) Engl.	31	61	
7	Lecythidaceae	<i>Bertholletia excelsa</i> Bonpl.	18	35	VU
8	Fabaceae	<i>Bowdichia</i> sp. Kunth	34	68	
9	Moraceae	<i>Brosimum parinarioides</i> Ducke	13	25	
10	Meliaceae	<i>Carapa guianensis</i> Aubl.	11	21	
11	Lecythidaceae	<i>Cariniana estrellensis</i> (Raddi) Kuntze	18	36	
12	Meliaceae	<i>Cedrela fissilis</i> Vell.	11	22	VU
13	Fabaceae	<i>Cedrelinga cateniformis</i> (Ducke) Ducke	33	65	
14	Boraginaceae	<i>Cordia goeldiana</i> Huber	18	36	
15	Lecythidaceae	<i>Couratari</i> sp. Aubl.	21	41	
16	Fabaceae	<i>Dipteryx</i> sp. Schreb.	14	27	
17	Vochysiaceae	<i>Erisma uncinatum</i> Warm.	29	58	
18	Myrtaceae	<i>Eucalyptus</i> sp. L'Hér.	14	27	
19	Myrtaceae	<i>Eugenia pyriformis</i> Cambess.	18	35	
20	Rutaceae	<i>Euxylophora paraensis</i> Huber	33	66	CR
21	Goupiaceae	<i>Goupia glabra</i> Aubl.	16	32	
22	Proteaceae	<i>Grevillea robusta</i> A. Cunn. ex R. Br.	24	48	
23	Bignoniaceae	<i>Handroanthus</i> sp. Mattos	17	33	
24	Fabaceae	<i>Hymenaea</i> sp. L.	16	32	
25	Fabaceae	<i>Hymenolobium petraeum</i> Ducke	14	28	
26	Fabaceae	<i>Hymenolobium</i> sp. Benth.	14	28	
27	Fabaceae	<i>Inga vera</i> Willd.	20	40	
28	Lauraceae	<i>Laurus nobilis</i> L.	18	36	
29	Fabaceae	<i>Machaerium paraguariense</i> Hassl.	19	37	
30	Fabaceae	<i>Machaerium</i> sp. Pers.	8	15	
31	Sapotaceae	<i>Manilkara elata</i> (Allemão ex Miq.) Monach.	20	39	
32	Meliaceae	<i>Melia azedarach</i> L.	24	47	
33	Lauraceae	<i>Mezilaurus itauba</i> (Meisn.) Taub. ex Mez	42	83	VU
34	Sapotaceae	<i>Micropholis venulosa</i> (Mart. & Eichler) Pierre	36	71	
35	Fabaceae	<i>Mimosa scabrella</i> Benth.	15	30	
36	Fabaceae	<i>Muellera campestris</i> (Mart. ex Benth.) M.J. Silva & A.M.G. Azevedo	20	39	
37	Fabaceae	<i>Myroxylon balsamum</i> (L.) Harms	27	53	
38	Lauraceae	<i>Nectandra megapotamica</i> (Spreng.) Mez	14	28	
39	Lauraceae	<i>Ocotea indecora</i> (Schott) Mez	18	36	
40	Lauraceae	<i>Ocotea porosa</i> (Nees & Mart.) Barroso	23	46	EN
41	Fabaceae	<i>Peltogyne</i> sp. Vogel	30	60	

Table 1 (continued)

Code	Family	Scientific Name	Samples	N	Category ^a
42	Pinaceae	<i>Pinus</i> sp. L.	21	42	
43	Sapotaceae	<i>Pouteria pachycarpa</i> Pires	24	47	
44	Simaroubaceae	<i>Simarouba amara</i> Aubl.	15	30	
45	Meliaceae	<i>Swietenia macrophylla</i> King	35	70	VU
46	Vochysiaceae	<i>Vochysia</i> sp. Aubl.	22	43	

^a Endangered species according to the category established by MMA Ordinance No. 443 of December 17, 2014 (MMA 2014). CR critically endangered, EN endangered, VU vulnerable

the matrix (Fig. 2c), producing a result, as shown in Fig. 2d; (4) LBP default: the new value of the center pixel will be a number (0–255) resulting from the sum of the values in Fig. 2d, i.e., $LBP = 1 + 8 + 32 + 128 = 169$. Finally, using the calculated values for each pixel in the image, a histogram of 256 patterns can be calculated and used as a representation of the image. The original LBP is invariant against any monotonous grayscale transformation, that is, as long as the order of pixel values remains the same, the output of the LBP operator remains constant (Ojala et al. 1994).

Despite the power to describe image textures, the LBP proposed in Ojala et al. (1994) is not rotation-invariant, an undesirable condition in certain applications (Pietikäinen et al. 2000). Rotation invariance implies that the same features of the image can still be extracted if the image is rotated to different angles. In 2000, to overcome the LBP invariance problem, Pietikäinen, Ojala, and Xu proposed a first version of LBP invariant rotation called LBPROT (Pietikäinen et al. 2000). Ojala et al. (2002) introduced a generalization of the LBP, where the 3×3 square neighborhood proposed in Ojala et al. (1994) was replaced by a neighborhood with P neighbors evenly distributed at an angle under a circle of radius R (Liu et al. 2017). Figure 3 depicts a generic representation of the extended LBP for situations with different values of parameters P and R . The mathematical formalization of the operator is defined in Eq. (1):

$$LBP_{P,R} = \sum_{p=0}^{P-1} s(g_p - g_c) 2^p \quad s(x) = \begin{cases} 1, & x \geq 0 \\ 0, & x < 0 \end{cases} \quad (1)$$

where R is the spatial resolution of the operator; P is the number of symmetrical circular neighbors; g_c is the gray-level intensity of the central pixel; g_p represents the gray level of neighboring pixels arranged in the circle; and $s(x)$ is the threshold function. Since the central pixel is located at the $g_c = (0,0)$ coordinate, then the neighborhood coordinates are given by (x_p, y_p) , where $x_p = -R \sin(2\pi p/P)$ and $y_p = -R \cos(2\pi p/P)$ (Ojala et al. 2002; Ahonen et al. 2009).

The non-rotation-invariant operator ($LBP_{P,R}$) is similar to the original LBP (Ojala et al. 1994). For example, if $P = 8$ and $R = 1$ are defined for the $LBP_{8,1}$ operator, there are basically two differences from the original LBP: (1) the pixels in the central pixel neighborhood are indexed to form a circular chain; and (2) the

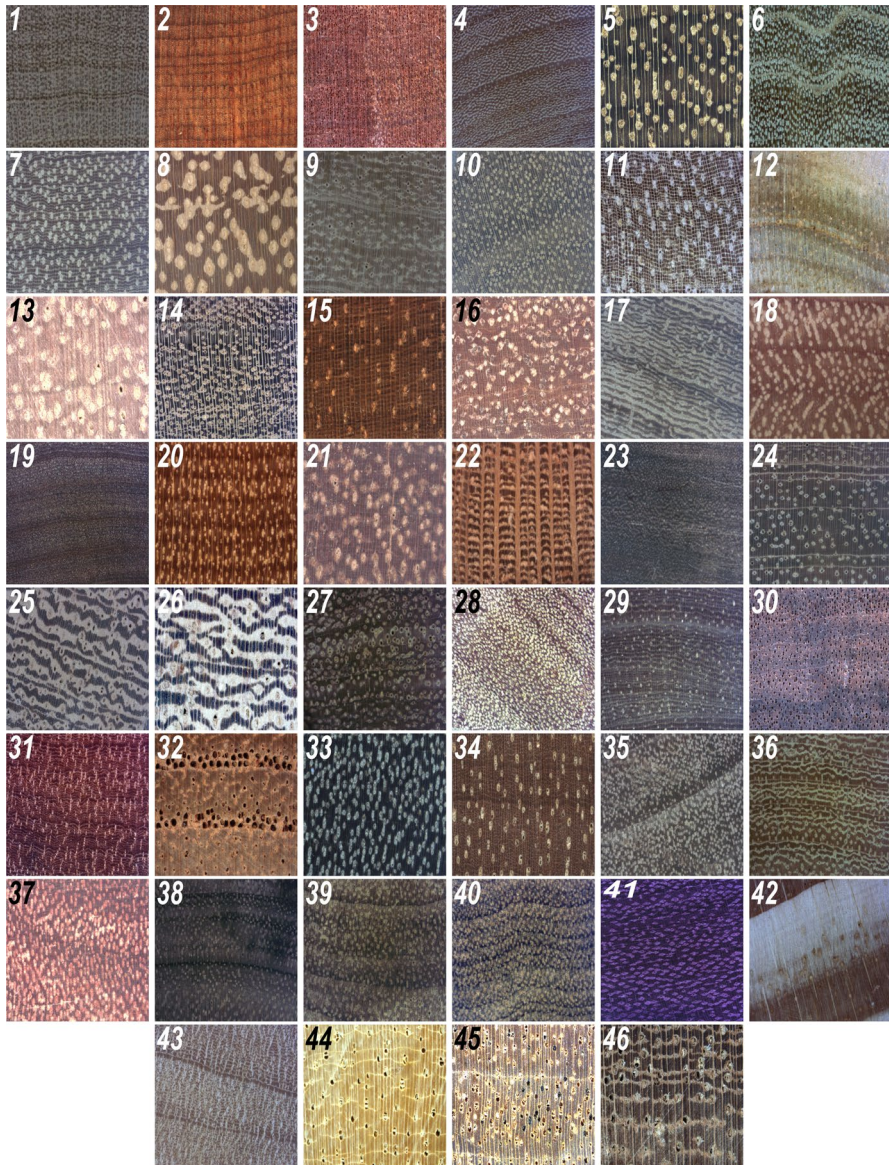


Fig. 1 Samples of macroscopic images of woods of species of Brazilian flora, including some endangered species. **Note:** The square images are for illustration purposes only. The processed images have a size of 2080×1540 pixels

gray-level values of diagonal pixels are determined by interpolation. For this situation, the four neighbors in the circle diagonal do not coincide with the centers of the pixels, thus justifying the use of bilinear interpolation. Similarly, the $LBP_{8,1}^{ri}$

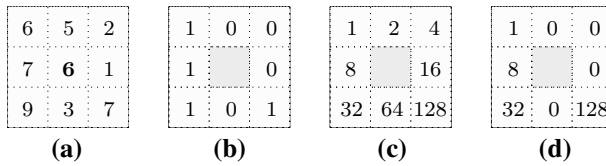


Fig. 2 Example of the original LBP method proposed in Ojala et al. (1994)

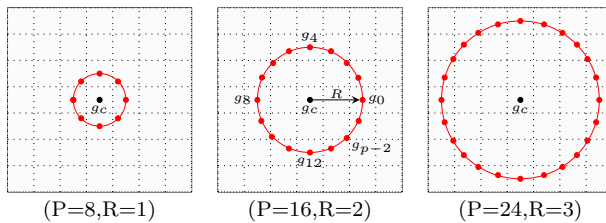


Fig. 3 Representation of the extended LBP method proposed in Ojala et al. (2002). When the location of the neighbors in the circle does not coincide with centers of the pixels, the gray values are determined by bilinear interpolation

operator is equivalent to LBPROT, but experiments have shown that this operator does not provide good discrimination (Pietikäinen et al. 2000; Ojala et al. 2002).

The main contribution of Ojala et al. (2002) was to recognize that some binary patterns occur more often than others (these patterns were called uniform). In practice, the operator called U is used to calculate the amount of spatial transitions (0–1 or vice versa) in a circular binary sequence (Ahonen et al. 2009). The pattern is “uniform” if $U \leq 2$; otherwise, it is non-uniform, and these are grouped under the same label. The most frequent and uniform binary patterns correspond to primitive micro-characteristics such as edges, corners, and points. Experimental results show that uniform patterns represent less than 90% of patterns in the vicinity (8,1) and about 70% in the vicinity (16,2) (Ojala et al. 2002).

The operators $LBP_{P,R}^{u2}$ and $LBP_{P,R}^{riu2}$ incorporate the concept of uniform patterns, and have the advantage of reducing the dimensionality of the feature vector while maintaining discriminative capacity. Therefore, the operators $LBP_{P,R}^{u2}$ and $LBP_{P,R}^{riu2}$ reduce the feature vector’s dimensionality from 2^P (standard LBP) to $P(P - 1) + 3$ and $P + 2$, respectively. The operator $LBP_{P,R}^{riu2}$ is uniform and rotation-invariant, and is formally defined in Eqs. (2) and (3) (Ojala et al. 2002):

$$LBP_{P,R}^{riu2} = \begin{cases} \sum_{p=0}^{P-1} s(g_p - g_c) & \text{if } U(LBP_{P,R}) \leq 2 \\ P + 1, & \text{otherwise} \end{cases} \quad (2)$$

$$\begin{aligned}
 U(\text{LBP}_{P,R}) = & \left| s(g_{P-1} - g_c) - s(g_0 - g_c) \right| \\
 & + \sum_{p=1}^{P-1} \left| s(g_p - g_c) - s(g_{p-1} - g_c) \right|.
 \end{aligned}
 \tag{3}$$

Materials and methods

Feature extraction and experiments

In this study, to cover aspects of spatial and angular resolution, three configurations of the uniform and rotation-invariant LBP operator ($\text{LBP}_{8,1}^{\text{riu}2}$, $\text{LBP}_{16,2}^{\text{riu}2}$, $\text{LBP}_{24,3}^{\text{riu}2}$) and three of the uniform and non-invariant rotation operator ($\text{LBP}_{8,1}^{\text{u}2}$, $\text{LBP}_{16,2}^{\text{u}2}$, $\text{LBP}_{24,3}^{\text{u}2}$) were considered. The color images were converted to 8-bit grayscale using the openCV function `cv2.cvtColor()` (`cv2.COLOR_BGR2GRAY` method). Afterward, LBP was used for feature extraction from grayscale macroscopic images. Feature extraction was done with the `local_binary_pattern()` function of the `scikit-image` library, available for the Python programming language. From each LBP descriptor configuration, histograms of texture pattern occurrences were obtained and normalized. The LBP feature histograms were used as inputs for supervised learning algorithms.

The first experimental approach was to use normalized individual LBP histograms as input sources for machine learning models. Then, two fusion schemes were considered: (a) early fusion and (b) late fusion. Basically, the schemes differ with respect to the level at which fusion is performed. Early fusion involves concatenation multiple histogram operators before the learning phase to create a new feature vector for multi-resolution analysis. For example, the combination $\text{LBP}_{8,1}^{\text{riu}2} + \text{LBP}_{16,2}^{\text{riu}2}$ results in a new vector with dimensionality: $10 + 18 = 28$. Late fusion is performed at the decision level of the classifiers. First, models are trained separately for each LBP feature set, and individual decisions are made. Then, a common decision is made by merging individual decisions. Here, the majority vote was used as a final decision rule. For the $\text{LBP}_{P,R}^{\text{u}2}$ operator, the feature space dimensionality increases by $P(P - 1) + 3$. For example, if $P=8$, the operator results in feature space with 59 vectors. However, if $P=16$ and $P=24$, the operator results in feature space with 243 and 555 vectors, respectively. Therefore, principal component analysis (PCA) was used to reduce the dimensionality of the feature spaces, except for $\text{LBP}_{8,1}^{\text{u}2}$. For the other configurations $\text{LBP}_{P,R}^{\text{u}2}$, the principal components that cumulatively explained 95% of the total variance of the original data (threshold = 0.95) were used as input vectors in the learning process of predictive models. The PCA was used to reduce the dimensionality of the feature space of the training set, and the obtained estimates were used to calculate the principal components for the hold-out samples. Figure 4 shows a simplified flowchart of the main steps of this study, as well as early and late fusion strategies.

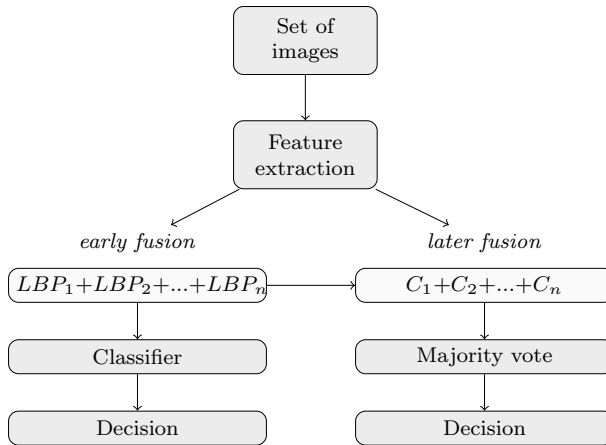


Fig. 4 Simplified flowchart of the main study steps, from the feature extraction step with different variants of the LBP method to the selection of the best species recognition model. Where: C_n : nth classifier trained with $LBP_{P,R}$ features

Algorithms, cross-validation, and evaluation metrics

In this study, three supervised learning algorithms were tested: (a) support vector machines (SVMs); (b) artificial neural networks (ANN); and (c) random forest (RF). Multilayer perceptron (MLP) networks were trained using the back-propagation algorithm (Venables and Ripley 2002). The grid search strategy was used to find the optimal tuning hyperparameters. First, for each machine learning algorithm, a grid of candidate hyperparameters was established. Then, the optimal tuning hyperparameters were found using repeated cross-validation. The hyperparameter variants for each machine learning algorithm and the respective packages are shown in Table 2. Classifiers were trained using the caret package (classification and regression training) (Kuhn et al. 2016). R language (version 3.5.3) was used to train classifiers and create graphics.

A common approach to estimate the expected performance of a predictive model is to implement some resampling method from the original data (Molinario et al. 2005; Kuhn and Johnson 2013). In this study, to obtain unbiased estimates of the performance of the machine learning algorithm variants, the repeated stratified k -fold cross-validation method (fivefold cross-validation, repeated ten times) was used. The cross-validation folds were created using stratified random sampling, whose stratification factor was the prediction classes. In the repeated k -fold CV, the learning data set is reorganized and divided into k -folds each new round of cross-validation (Refaeilzadeh et al. 2009). More specifically, the complete data set was divided into five subgroups of approximately equal and distinct sizes, with representatives of all species in each subgroup. This procedure was repeated ten times. Repeating the resampling can produce very different values, but if applied enough will efficiently estimate the true value (Kuhn and Johnson 2013).

Table 2 Candidate hyperparameters for each machine learning algorithm and libraries used

Algorithm	Hyperparameter variants	Method/Package	Author
Support Vector Machine (SVM)	Degree = c(2,3) C = 2 ^{seq} (-2,12,1) Scale = C(0.001, 0.005, 0.01, 0.02, 0.05, 0.1) Size = seq(1,9,1) Decay = seq(0.001, 0.007, 0.001)	svmPoly/kernlab	Karatzoglou et al. (2004)
Artificial Neural Network (ANN)	ntrree = C(500, 1000, 1500, 2000) mtry = C(2:max _p)	nnet/nnet	Venables and Ripley (2002)
Random Forest (RF)		rfr/randomForest	Liaw et al. (2002)

Where: SVM = Support Vector Machine; ANN = Artificial Neural Networks; RF = Random Forest; degree = kernel parameter; scale = scaling parameter of the kernel polynomial; C = cost of constraints violation; size = number of neurons in the hidden layer; decay = parameter for weight decay; mtry = number of predictors used in the construction of each tree (max_p: maximum number of predictors; this depends on the feature space considered); ntrree = number of trees to grow

Unfortunately, it was not possible to control the experiment, so that the images from the same block were not in the training and validation set. This information was not stored properly during the collection of the images (or it was lost). It could be assumed that two images of the same block were made in the sequence, that is, two images were not obtained in the same position of the block. Even so, many images were excluded due to the presence of grooves (or other reasons). This is important information for this type of experiment that we intend to control in future research. It is emphasized that this dataset was assembled over many years and the main purpose was to visualize macroscopic characteristics of the woods (parenchyma, rays, pores, among others) in the context of anatomical identification.

In the repeated cross-validation method, confusion matrices were computed for each cross-validation fold (hold-out samples). Then, a simple confusion matrix was calculated by adding the 50 matrices determined on the hold-out samples. This confusion matrix that gathers all out-of-sample predictions was used to evaluate the confusion between species by the most accurate classifier. The performance metrics of the classifiers were extracted using the confusionMatrix() function of the caret package, which generates the confusion matrix and numerous metrics using the one versus all approach. The overall accuracy of the system was calculated by Eq. (4). Due to class imbalance, the Recall (Eq. 5) and F1-score ($\beta = 1$) (Eq. 6) metrics were obtained for greater reliability of the performance estimation. The precision was obtained by Eq. 7:

$$Accuracy = \frac{TP + TN}{TP + FP + TN + FN} \quad (4)$$

$$Recall = \frac{TP}{TP + FN} \quad (5)$$

$$F1\text{-score} = (1 + \beta^2) \frac{Precision \cdot Recall}{[(\beta^2 \cdot Precision) + Recall]} \quad (6)$$

$$Precision = \frac{TP}{TP + FP} \quad (7)$$

where True positive (TP) = number of correctly classified samples in class C_i ; True negative (TN) = number of samples correctly classified as not belonging to class C_i ; False positive (FP) = number of misclassified samples in class C_i ; False negative (FN) = number of samples misclassified as not belonging to class C_i . All these metrics were also computed for each hold-out sample, and then, a final average was calculated as an estimate of the classifier's performance. The variance of performance metrics was also estimated in repeated cross-validation folds.

Table 3 Performance of the classifiers in repeated cross-validation using the uniform and rotation-invariant LBP method (LBP_{PR}^{u2}), with and without concatenation of operators (early fusion)

Classifier	P,R	Vector Size	Statistics	10x5-folds cross-validation							
				SVM ^a			ANN (MLP)			RF	
				Accuracy	F1-Score	F1-Score	Accuracy	F1-Score	F1-Score	Accuracy	F1-Score
C1	8,1	10	Mean	89.97	87.73	90.99	89.11	77.41	74.96		
			Sd	1.27	1.59	1.24	1.61	2.05	2.43		
			Min.	86.68	83.48	87.99	84.77	73.37	70.57		
			Max.	92.06	90.86	93.92	92.21	81.68	80.08		
C2	16,2	18	Mean	93.37	91.98	93.96	92.68	76.24	74.1		
			Sd	1.03	1.29	0.9	1.23	1.87	1.82		
			Min.	90.86	89.14	92.43	90.08	72.44	71.58		
			Max.	96.08	94.68	96.01	95.21	79.89	77.64		
C3	24,3	26	Mean	94.67	93.5	94.56	93.57	75.45	73.32		
			Sd	0.89	1.07	1.02	1.31	1.86	1.03		
			Min.	92.84	91.63	92.55	90.3	70.74	72.02		
			Max.	96.31	95.49	96.33	95.91	79.63	74.28		
C4	8,1 + 16,2	28	Mean	95.3	94.1	95.24	94.19	84.04	82.02		
			Sd	0.94	1.2	1.00	1.21	1.46	1.78		
			Min.	93.47	91.25	93.12	92.02	81.48	79.31		
			Max.	97.12	96.33	97.12	96.3	87.66	85.26		
C5	8,1 + 24,3	36	Mean	95.93	95.02	96.02	95.12	84.8	82.66		
			Sd	0.88	1.12	0.87	1.16	1.57	1.77		
			Min.	93.7	92.27	93.62	91.69	81.1	78.98		
			Max.	98.41	97.79	97.61	97.13	87.53	85.68		

Table 3 (continued)

Classifier	P,R	Vector Size	Statistics	10x5-folds cross-validation							
				SVM ^d			ANN (MLP)			RF	
				Accuracy	F1-Score	F1-Score	Accuracy	F1-Score	F1-Score	Accuracy	F1-Score
C6	16,2 + 24,3	26	Mean	97.29	96.75	95.71	94.77	79.54	77.34		
			Sd	0.78	0.97	0.83	1.1	1.69	2.03		
			Min.	95.29	93.72	93.98	92.59	75.33	72.97		
C7	8,1 + 16,2 + 24,3	36	Max.	98.69	98.41	97.64	97.11	83.2	80.28		
			Mean	98.07	97.67	96.45	95.58	84.96	83.02		
			Sd	0.66	0.79	0.99	1.33	1.62	1.96		
			Min.	96.61	95.52	93.12	92.14	81.36	79.21		
			Max.	99.47	99.33	98.15	97.82	88.25	87.1		

Where: *P* number of symmetrical circular neighbors, *R* spatial resolution of the operator, *SVM* support vector machine, *ANN* artificial neural networks, *RF* random forest, *MLP* multilayer perceptron, *Sd* standard deviation in resampling, *Min.* minimum, *Max.* maximum

^dPolynomial kernel. All measures are expressed as a percentage

Table 4 Performance of the classifiers in repeated cross-validation using the uniform and non-rotation-invariant LBP method (LBP_{pr}^{u2}), with and without concatenation of operators (early fusion)

Classifier	P,R	Vector size	Statistics	10x5-folds cross-validation							
				SVM ^u			ANN (MLP)			RF	
				Accuracy	F1-Score	F1-Score	Accuracy	F1-Score	F1-Score	Accuracy	F1-Score
C1	8,1	59	Mean	92.65	90.6	91.58	89.82	86.55	83.83		
			Sd	1.19	1.52	1.41	1.73	1.42	1.75		
			Min.	89.76	87.33	88.74	85.31	83.29	80.22		
			Max.	95.5	94.31	93.99	93.04	89.18	87.34		
C2	16,2	243 (13)	Mean	93.44	92.05	88.18	86.45	90.22	89.04		
			Sd	1.22	1.51	1.69	1.88	1.46	1.71		
			Min.	91.27	89.21	83.86	81.94	86.09	84.28		
			Max.	96.04	94.97	91.41	89.96	92.97	92.85		
C3	24,3	555 (17)	Mean	95.53	94.66	90.31	89.07	91.05	89.85		
			Sd	1.04	1.26	1.41	1.68	1.49	1.68		
			Min.	93.47	91.53	87.23	84.74	86.82	84.45		
			Max.	97.88	97.5	94.5	94.02	93.75	93.12		
C4	8,1 + 16,2	302 (13)	Mean	94.84	93.37	91.52	89.88	91.6	90.42		
			Sd	1.05	1.47	1.26	1.47	1.26	1.47		
			Min.	92.37	89.51	88.05	85.8	88.98	87.72		
			Max.	97.1	96.38	94.18	93.0	93.92	93.55		
C5	8,1 + 24,3	614 (17)	Mean	95.76	94.79	92.46	91.24	91.86	90.87		
			Sd	1.11	1.29	1.13	1.35	1.1	1.38		
			Min.	93.44	91.6	90.48	88.93	88.63	86.75		
			Max.	97.88	97.8	95.24	94.59	93.68	93.18		

Table 4 (continued)

Classifier	P,R	Vector size	Statistics	10x5-folds cross-validation					
				SVM ^a		ANN (MLP)		RF	
				Accuracy	F1-Score	Accuracy	F1-Score	Accuracy	F1-Score
C6	16,2 + 24,3	798 (17)	Mean	95.76	94.67	91.6	90.29	90.48	89.31
			Sd	0.96	1.22	1.41	1.58	1.31	1.58
			Min.	92.95	90.79	88.03	86.66	86.82	84.65
			Max.	97.36	96.84	94.75	93.99	92.97	91.8
C7	8,1 + 16,2 + 24,3	857 (17)	Mean	96.03	95.15	91.89	90.66	91.4	90.2
			Sd	0.85	1.03	1.26	1.57	1.25	1.55
			Min.	93.47	91.52	89.1	87.0	88.03	86.65
			Max.	97.66	97.18	95.25	94.79	93.49	93.04

Where: *P* number of symmetrical circular neighbors, *R* spatial resolution of the operator, *SVM* support vector machine, *ANN* artificial neural networks, *RF* random forest, *MLP* multilayer perceptron

^aOn the left is the size of the feature space obtained with the LBP operator and in parentheses the number of principal components that cumulatively explained 95% of the total variation of the original data. The principal components were used as input vectors in the learning process of predictive models, reducing the computational cost

^bPolynomial kernel. *Sd* standard deviation in resampling, *Min.* minimum, *Max.* maximum. All measures are expressed as a percentage

Results and discussion

Classifier performance

Tables 3 and 4 show the performance estimates and standard deviations in the cross-validation (fivefold cross-validation, repeated ten times), for the classifiers constructed using feature spaces $LBP_{P,R}^{riu2}$ and $LBP_{P,R}^{u2}$, respectively. The results found using the $LBP_{P,R}^{u2}$ and $LBP_{P,R}^{riu2}$ operators showed that individual LBP texture patterns extracted from macroscopic images of the wood provide good information for species discrimination, and that when concatenated, improve classifier performance. It was found that the Artificial Neural Network (ANN) and Support Vector Machine (SVM) algorithms showed better learning ability based on LBP texture patterns.

The strategy of concatenating uniform and rotation-invariant LBP histograms with different resolutions ($LBP_{8,1}^{riu2} + LBP_{16,2}^{riu2} + LBP_{24,3}^{riu2}$) provided the learning of more accurate classifiers, for all considered algorithms. The average F1-score in the cross-validation was 97.67% using SVM classifier (degree = 3, scale = 0.001, $C = 2^{11}$; classifier C_7 in Table 3). This was the most accurate classifier using the early fusion strategy. The use of this SVM classifier resulted in 4.17% increases in F1-score, compared to the performance of the best SVM classifier built using individual LBP histograms ($LBP_{24,3}^{riu2}$). Likewise, this SVM classifier outperformed the best ANN and random forest (RF) classifiers. The average F1-score was 2.09 and 14.65% points higher for this SVM classifier compared to the best ANN and RF classifiers, respectively.

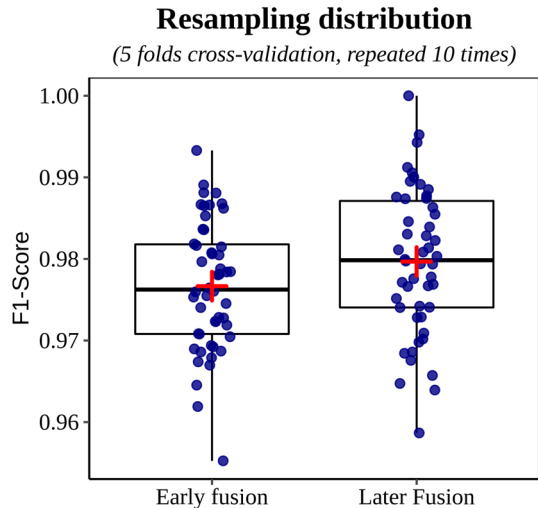
The concatenation of features from the non rotation-invariant LBP also showed good results. The average F1-score in the cross-validation was 95.15% using SVM classifier (degree = 2, scale = 0.05, $C = 4$; classifier C_7 in Table 4). However, the estimated average F1-score of this classifier was 2.52% points less than the best classifier learned from rotation-invariant LBP features. We identified that the best RF classifiers were built from non rotation-invariant LBP features.

The classifier combination strategy (late fusion) aimed to use the strengths inherent in each classifier, seeking to improve the recognition system. Despite this, the best combination of classifiers resulted in an increase of only 0.33% point in the F1-score (98%) compared to the more accurate classifier using the early fusion strategy. This classifier was obtained by combining four SVM classifiers from Tables 3 (C_6 , C_7) and 4 (C_2 , C_7) and one ANN (MLP) classifier from Table 3 (C_7). It was found that most classifiers showed a tendency to incorrectly predict the same observations in the hold-out sample. This was the most likely reason for the little improvement found.

Box plot comparing the distributions of the F1-score metric in repeated cross-validation using the most accurate early fusion and late fusion classifiers is shown in Fig. 5. These classifiers presented a coefficient of variation less than 1% for the metric F1-score, which indicate the stability of both to predict future samples (not used to build the classifier).

The problem of recognizing forest species from wood images (macroscopic or microscopic) has been addressed by other scientific studies. Studies often evaluate

Fig. 5 Box plot comparing the distributions of the F1-score metric in repeated cross-validation using the most accurate early fusion and late fusion classifiers. Vertical bars represent $Q1 - 1.5 \cdot IQR$ (1st quartile minus 1.5 times the interquartile range) and $Q3 + 1.5 \cdot IQR$ (3rd quartile plus 1.5 times the interquartile range); the cross represents the average performance



different image capture techniques, feature extraction methods [color features, Gray-Level Co-occurrence Matrix (GLCM), Gabor filters, Local Binary Patterns (LBP), Fractals, Local Phase Quantization, and others] and their combinations, machine learning techniques (especially SVM and ANN) and convolutional neural networks (CNN) (e.g., Khalid et al. 2008; Nasirzadeh et al. 2010; Yusof et al. 2013; Paula Filho et al. 2014; Hafemann et al. 2014; Martins et al. 2015; Yadav et al. 2015; Ibrahim et al. 2016; Siew et al. 2017; Kobayashi et al. 2017; Ravindran et al. 2018; Figueroa-Mata et al. 2018; Kobayashi et al. 2019).

Khalid et al. (2008) developed a system for automatic recognition of tropical species from macroscopic wood images ($n = 1949$) based on the feature extractor GLCM and ANN (MLP network). This system showed an accuracy greater than 95% for the recognition of 20 species of tropical wood. Nasirzadeh et al. (2010) designed a recognition system based on the nearest-neighbor classifier and local binary pattern histograms extracted from enhanced wood images of 37 tropical species. The experiments carried out revealed greater accuracy using the Histogram Fourier feature (96.6% and 100%) with $P = 24$ and $R = 3$.

Similar to the present study, the operator $LBP_{P,R}^{u2}$ was among the operators chosen by Paula Filho et al. (2014) to search for species recognition from macroscopic images of wood, for offering good discrimination characteristics. The classifiers trained using the SVM algorithm and non rotation-invariant LBP histogram were less accurate than those reported in this study. The best recognition rate found in the study by Paula Filho et al. (2014) was 97.77%, using a combination of classifiers trained on different descriptors. The $LBP_{P,R}^{riu2}$ patterns extracted from macroscopic wood images in the present study also provided robust information for classifiers, ensuring high species recognition rates. Using the $LBP_{P,R}^{riu2}$ descriptor over $LBP_{P,R}^{u2}$ provides computational advantage by reducing the dimensionality of the LBP feature vector. For example, for $LBP_{8,1}^{u2}$, the feature vector dimension is 59, but decreases to 10 ($P + 2$) using the $LBP_{8,1}^{riu2}$ operator. The increase in P makes the

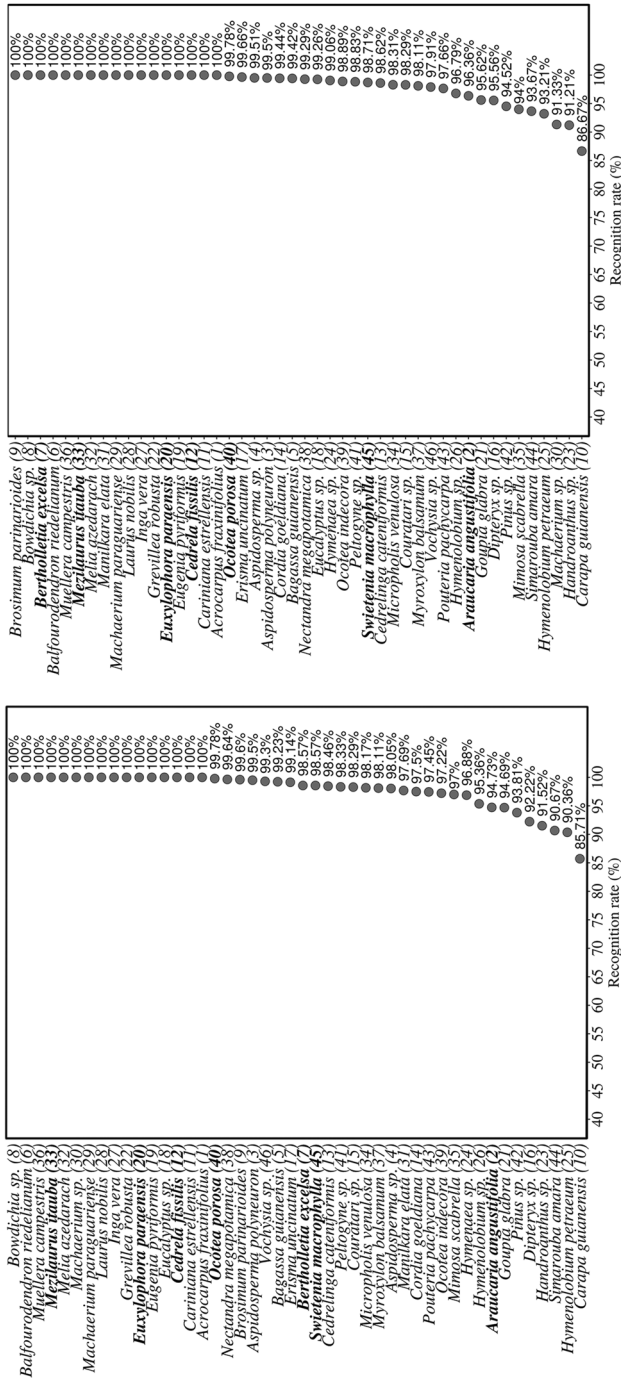


Fig. 6 Average recall (recognition rate by species) in repeated cross-validation using the most accurate early fusion and late fusion classifiers. The endangered species included in the official list of Brazil are highlighted in bold

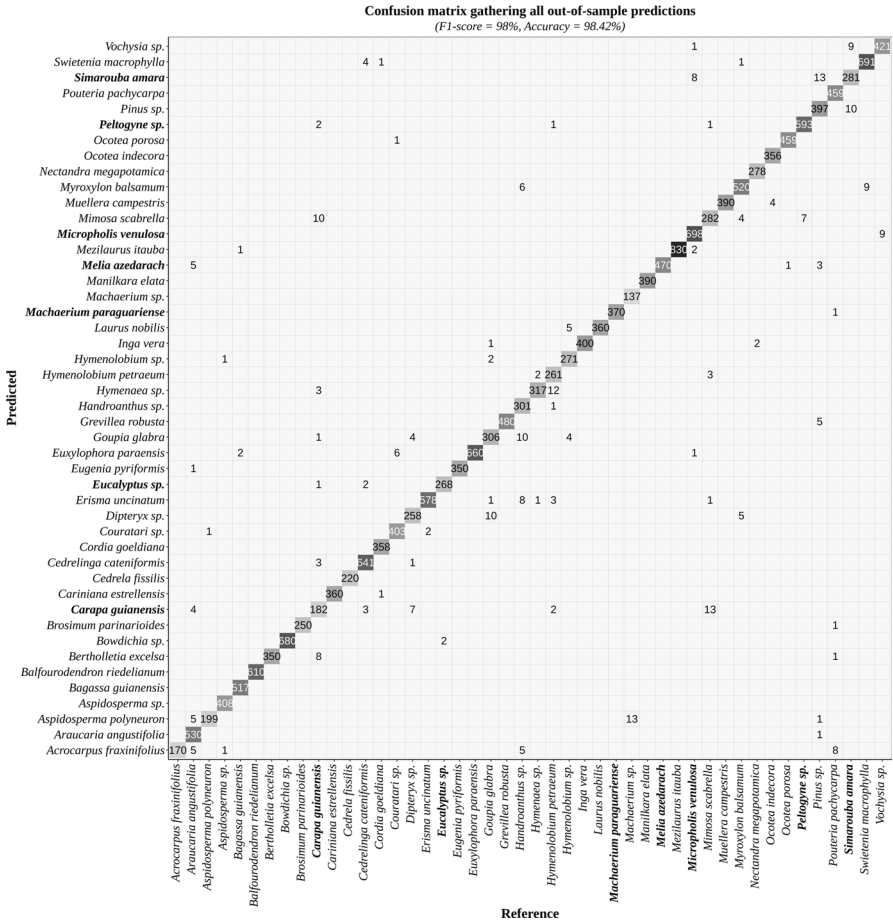


Fig. 7 Confusion matrix gathering all out-of-sample predictions in repeated cross-validation for the late fusion classifier. The endangered species included in the official list of Brazil are highlighted in bold

discrepancy between operators in relation to the vector size even greater. In addition, $LBP_{P,R}^{riu2}$ is rotation-invariant, an important property that increases the classification system's ability to predict nature.

Figure 6 shows the average recall per species (true positives rate per species) for hold-out samples in repeated cross-validation. The best early fusion classifier (SVM classifier in Table 3) showed a 100% recognition rate for 16 species, including three from Brazil's official list of endangered species (*Mezilaurus itauba*, *Euxylophora paraensis*, and *Cedrela fissilis*) (Fig. 6a). The fusion of classifiers improved the average recall of some species. For example, all samples of wood images from *Bertholletia excelsa* were recognized correctly. This species is also listed as endangered. Only *Carapa guianensis* showed an average recall of less than 90%. The fusion of classifiers increased the average recall of this species by almost 1% point (Fig. 6b).

Misclassification and wood anatomical features on transversal surface

The quality of a classifier's predictions can be verified by examining its confusion matrix (CM). The CM for the late fusion classifier is shown in Fig. 7. This confusion matrix gathers all out-of-sample predictions ($n = 19,010$) in repeated cross-validation. This experiment revealed that more than 50% of the species showed no misclassifications or occurred only once or twice. These results are very promising, especially when considering the endangered species of Brazilian flora.

However, it is pointed out that in a quick analysis, for example, a wood anatomist would not confuse *Aspidosperma polyneuron* wood (pink) with *Aspidosperma* sp. (yellow color). On the other hand, there are groups that are possible to be confused even by specialists in wood anatomy, but which presented satisfactory results when analyzing the classifier's behavior.

In this study, several species which are confused in practice due to the similarities of the anatomical characteristics were correctly classified by the proposed system. These species are divided into 4 main groups:

- (i) **Group 1:** This group is composed of the species *Simarouba amara* and *Brosimum parinarioides*. The confusion occurs mainly when the wood is transformed into laminated wood, because the two species have confluent aliform parenchyma.
- (ii) **Group 2:** The wood of the species *Bertholletia excelsa* and *Cariniana estrellensis*, are confused, because both have reticulate parenchyma. In this case, the absence of confusion by the system is even more advantageous, as the species *Bertholletia excelsa*, in addition to being protected from exploitation by Brazilian legislation, is also on the list of the Convention on the International Trade in Endangered Species (CITES).
- (iii) **Group 3:** This group is formed by the species of Lauraceae (*Ocotea indecora*, *Ocotea porosa*, and *Nectandra megapotamica*), which have a great similarity, often making it impossible to differentiate due to the characteristics of the anatomical structure.
- (iv) **Group 4:** This group is formed by the species *Cedrela fissilis*, *Swietenia macrophylla*, *Carapa guianensis*, and *Cedrelinga cateniformis*. Again, the presence of species (*Cedrela fissilis* and *Swietenia macrophylla*) in the extinction list further justifies the potential use of the system.

Ravindran et al. (2018) trained Convolutional Neural Networks (CNN), at the species and genus levels, to recognize woods of Neotropical species of the Meliaceae family. The data set used included sample images of *Cedrela fissilis* and *Swietenia macrophylla* wood, which is also presented in the present study and listed on CITES. At the species level, the learned CNN classifier showed confusion (approximately 20%) between *Cedrela fissilis* and *Cedrela odorata*. The recognition rate for *Swietenia macrophylla* was approximately 91%, being confused with *Carapa guianensis* and *Swietenia mahagoni*. In the present study, *Cedrela fissilis* and *Swietenia macrophylla* had 100% and 98.71%, respectively, of their images recognized correctly by the late fusion classifier.

Finding reasonable explanations for the system's misclassifications based on the anatomical characteristics of the transversal surface of the wood is not simple. Despite this, it is believed that similarities in the anatomical structures of the transversal section may explain, at least in part, the misclassifications among some species. For example, we found in Fig. 6b that *Carapa guianensis* showed less sensitivity (or recall). This species was mostly misclassified as *Mimosa scabrella* or *Bertholletia excelsa*. Likewise, *Mimosa scabrella* was sometimes misclassified as *Carapa guianensis*. These misclassifications may be associated with the similarity of the anatomical structure of these species, as they all have diffuse porosity, average pore diameter between 100 and 200 μm and fiber wall thickness between thin and thick (Détienne and Jacquet 1983; Fedalto et al. 1989; Marchiori 1995; Miller and Détienne 2001; Lens et al. 2007; White and Gasson 2008; Muñiz et al. 2012; Carreras et al. 2012; Bhikhi et al. 2016).

Handroanthus sp. showed the second-highest misclassification rate. This species was most often misclassified as *Goupia glabra* or *Erisma uncinatum*. These species have anatomical similarities, such as diffuse porosity, on average between 5 and 20 pores per square millimeter, rays with an average width between 1 and 3 cells, average between 4 and 12 rays per linear millimeter (Kribs 1968; Détienne and Jacquet 1983; Berti and Abbate 1992; Miller and Détienne 2001; Richter and Dallwitz 2009; Pace and Angyalossy 2013; Bhikhi et al. 2016).

Machaerium sp. was misclassified only as *Aspidosperma polyneuron*. Again, similar anatomical characteristics are observed among the woods of these species, such as diffuse porosity, the average pore diameter between 50 and 100 μm , between 40 and 100 pores per square millimeter and the presence of diffuse-in-aggregates axial parenchyma (Tortorelli 1956; Détienne and Jacquet 1983).

Other species showed lower misclassification rates when considering the total number of out-of-sample predictions by species. For example, of the 280 images of *Hymenolobium petraeum* included in the hold-out samples, the classifier predicted only 12 (4.3%) as *Hymenaea* sp. The literature also reports similarities between the characteristics of the anatomical structure of these species, such as diffuse porosity, pores with an average diameter greater than 200 μm , an average of less than 5 pores per square millimeter, cell wall of the fibers classified from thin to thick, axial parenchyma types: aliform, lozenge-aliform, confluent, and marginal, among other characteristics (PROTA 2002; Détienne and Jacquet 1983; Miller and Détienne 2001; Richter and Dallwitz 2009).

Likewise, a few samples of *Simarouba amara* ($n = 300$) were misclassified as *Pinus* sp. (3.3%) or *Vochysia* sp. (3%). First, it is important to emphasize that *Pinus* sp. belongs to Gymnosperms and its anatomical structure is mostly composed of tracheids, rays, and resin canals. On the other hand, *Simarouba amara* and *Vochysia* sp. are classified as Angiosperms, presenting in their structure mainly fibers, pores, rays, and axial parenchyma. Thus, *Simarouba amara* and *Pinus* sp., despite presenting different anatomical structures, constitute elements that have certain structural similarities, such as tracheids that resemble fibers and resin canals that are similar to pores. It is possible that this fact contributed to the confusion between these species. *Simarouba amara* and *Vochysia* sp. also have high similarity in their anatomical structure, sharing characteristics such as

diffuse porosity, average less than five pores per square millimeter, fiber wall with thickness classified as thin to thick, axial parenchyma aliform, confluent, and others (Mainieri 1958; Quirk 1980; Détienne and Jacquet 1983; Fedalto et al. 1989; Berti and Abbate 1992; Miller and Détienne 2001; Muñiz et al. 2012).

Conclusion

The Local Binary Patterns texture descriptor extracted from macroscopic images of wood samples provides excellent information for species discrimination. The use of histograms of simple LBP operators with the powerful supervised learning algorithms such as SVM and ANN allowed the construction of classifiers with F1-score higher than 90%, in most cases.

The concatenation strategy of $LBP_{P,R}^{riu2}$ operators (early fusion) enabled multi-resolution analysis and generally contributed to increase the accuracy of the classifiers, reaching F1-score of 97.67%. Similarly, the approach of classifier combination (late fusion) was able to improve the system F1-score by 0.33% point compared to the early fusion strategy.

It was identified that some groups of species (group 1, group 2, group 3, and group 4) present in this study, which are generally confused by specialists in wood anatomy, were perfectly differentiated by our classification system.

The results here of using computer vision for the recognition of forest species from macroscopic images of wood were effective, and if combined with traditional identification mechanisms and empirical experience, it can be an important tool to minimize identification errors of species of Brazilian flora, in particular endangered species, for which the proposed classification system showed high accuracy.

Acknowledgements We thank the Laboratory of Anatomy and Wood Quality (LANAQM) of Federal University of Paraná (UFPR) for making data available. This study was financed in part by the Coordenação de Aperfeiçoamento de Pessoal de Nível Superior—Brazil (CAPES)—Finance Code 001 and by the Conselho Nacional de Desenvolvimento Científico e Tecnológico (CNPq).

Compliance with ethical standards

Conflict of interest The authors declare that they have no known competing financial interests or personal relationships that could have appeared to influence the work reported in this paper.

References

- Ahonen T, Matas J, He C, Pietikäinen M (2009) Rotation invariant image description with local binary pattern histogram fourier features. In: Scandinavian Conference on Image Analysis, Springer Berlin Heidelberg, pp 61–70, https://doi.org/10.1007/978-3-642-02230-2_7
- Berti RN, Abbate ME (1992) Legnami tropicali importati in italia: Anatomia e identificazione (Tropical timber imported into Italy: Anatomy and identification). volume ii: Latin america

- Bhikhi CR, Maas PJM, Koek-Noorman J, van Andel TR (2016) Timber Trees of Suriname. LM Publishers, Volendam, Países Baixos
- Bila NF, Luis R, Gonçalves TAP, de Muñiz GIB, Nisgoski S (2018) Wood anatomy of five species from mozambique and its potential application. *Bosque* 39(2):169–175. <https://doi.org/10.4067/s0717-92002018000200169>
- Carreras R, Cuza A, Teruel J, González LR (2012) Árboles y maderas de Baracoa, Cuba (Trees and woods from Baracoa, Cuba). Publicitat Tafanet, Spain
- Costa MLM, Bajgielman T, Pereira TS, Maurenza D, Amaro R, Dalcin EC, Maunder M (2016) Estratégia nacional para a conservação ex situ de espécies ameaçadas da flora brasileira (National strategy for the ex situ conservation of endangered species of Brazilian flora). Centro Nacional de Conservação da Flora — CNC Flora: Jardim Botânico do Rio de Janeiro: Andrea Jakobsson, Rio de Janeiro. 24 p
- Deklerck V, Mortier T, Goeders N, Cody RB, Waegeman W, Espinoza E, Acker JV, den Bulcke JV, Beeckman H (2019) A protocol for automated timber species identification using metabolome profiling. *Wood Sci Technol* 53(4):953–965. <https://doi.org/10.1007/s00226-019-01111-1>
- Détienne P, Jacquet P (1983) Atlas d'identification des bois de l'Amazonie et des régions voisines (Identification Atlas of the woods of the Amazon and neighboring regions). GERDAT-CTFT
- Fedalto LC, Mendes I, Coradin VTR (1989) Madeiras da Amazônia, descrição do lenho de 40 espécies ocorrentes na Floresta Nacional do Tapajós (Timber from the Amazon, description of the wood of 40 species occurring in the Tapajós National Forest). Tech. rep, Brazilian Institute of the Environment and Renewable Natural Resources
- Figueroa-Mata G, Mata-Montero E, Valverde-Otarola JC, Arias-Aguilar D (2018) Using deep convolutional networks for species identification of xylotheque samples. In: 2018 IEEE International Work Conference on Bioinspired Intelligence (IWOB1), IEEE, <https://doi.org/10.1109/iwobi.2018.8464216>
- Forzza RC, Leitman PM, Costa A, Carvalho Jr AAd, Peixoto AL, Walter BMT, Bicudo C, Zappi D, Costa DPd, Lleras E, et al. (2010) Catálogo de plantas e fungos do Brasil-Vol. 1 (Catalog of plants and fungi from Brazil-Vol. 1). JBRJ
- Hafemann LG, Oliveira LS, Cavalin P (2014) Forest species recognition using deep convolutional neural networks. In: 2014 22nd International Conference on Pattern Recognition, IEEE, <https://doi.org/10.1109/icpr.2014.199>
- He DC, Wang L (1990) Texture unit, texture spectrum, and texture analysis. *IEEE Trans Geosci Remote Sens* 28(4):509–512. <https://doi.org/10.1109/igarss.1989.575836>
- IBÁ (2016) Relatório anual ibá 2016 (Ibá 2016 annual report)
- Ibrahim I, Khairuddin ASM, Talip MSA, Arof H, Yusof R (2016) Tree species recognition system based on macroscopic image analysis. *Wood Sci Technol* 51(2):431–444. <https://doi.org/10.1007/s00226-016-0859-4>
- Karatzoglou A, Smola A, Hornik K, Zeileis A (2004) kernlab—an s4 package for kernel methods in r. *J Stat Softw* 11(9):1–20. <https://doi.org/10.18637/jss.v011.i09>
- Khalid M, Lee ELY, Yusof R, Nadaraj M (2008) Design of an intelligent wood species recognition system. *Int J Simul Syst Sci Technol* 9(3):9–19
- Kobayashi K, Hwang SW, Lee WH, Sugiyama J (2017) Texture analysis of stereograms of diffuse-porous hardwood: identification of wood species used in tripitaka koreana. *J Wood Sci* 63(4):322–330. <https://doi.org/10.1007/s10086-017-1625-4>
- Kobayashi K, Hwang SW, Okochi T, Lee WH, Sugiyama J (2019) Non-destructive method for wood identification using conventional x-ray computed tomography data. *J Cult Herit* 38:88–93. <https://doi.org/10.1016/j.culher.2019.02.001>
- Kribs DA (1968) Commercial foreign woods on the American market. Dover Publications, New York
- Kuhn M, Johnson K (2013) Applied predictive modeling, vol 810. Springer, New York
- Kuhn M, Wing J, Weston S, Williams A, Keefer C, Engelhardt A, Cooper T, Mayer Z, Kenkel B, Team R, et al. (2016) CARET: Classification and regression training. In: R package version 6.0–21. CRAN, Vienna, Austria
- Kuo TY, Wang WC (2019) Determination of elastic properties of latewood and earlywood by digital image analysis technique. *Wood Sci Technol* 53(3):559–577. <https://doi.org/10.1007/s00226-019-01096-x>
- Lens F, Baas P, Jansen S, Smets E (2007) A search for phylogenetically informative wood characters within lecythidaceae s.l. *Am J Bot* 94(4):483–502. <https://doi.org/10.3732/ajb.94.4.483>
- Liaw A, Wiener M, et al. (2002) Classification and regression by randomforest. *R news* 2(3):18–22, Accessed: 2019-09-17 01:53:28

- Liu L, Fieguth P, Guo Y, Wang X, Pietikäinen M (2017) Local binary features for texture classification: taxonomy and experimental study. *Pattern Recognit* 62:135–160. <https://doi.org/10.1016/j.patco.2016.08.032>
- Mainieri C (1958) I-Madeiras Denominadas Caixeta (I-Woods Named Caixeta Brazil). Instituto de Pesquisas Tecnológicas, São Paulo, Brazil. Publicação no. 572
- Marchiori JNC (1995) Anatomia da madeira e casca da bracinga, mimosa scabrella benth. Anatomy of wood and bark of bracinga, mimosa scabrella benth). *Sci Nat* 17(17):115. <https://doi.org/10.5902/2179460x26536>
- Martinelli G, Moraes MA (2013) Livro vermelho da flora do Brasil (Red book on the flora of Brazil). CNCFIora, National Center for Flora Conservation Rio de Janeiro
- Martins J, Oliveira L, Nisgoski S, Sabourin R (2013) A database for automatic classification of forest species. *Mach Vis Appl* 24(3):567–578. <https://doi.org/10.1007/s00138-012-0417-5>
- Martins J, Oliveira LS, Britto A, Sabourin R (2015) Forest species recognition based on dynamic classifier selection and dissimilarity feature vector representation. *Mach Vis Appl* 26(2–3):279–293. <https://doi.org/10.1007/s00138-015-0659-0>
- Maruyama T, Oliveira L, Britto A Jr, Nisgoski S (2018) Automatic classification of native wood charcoal. *Ecol Inform* 46:1–7. <https://doi.org/10.1016/j.ecoinf.2018.05.008>
- Miller RB, Détienne P (2001) Major timber trees of Guyana: wood anatomy. The Tropenbos Foundation, Wageningen, <https://www.tropenbos.org/resources/publications>
- MMA (2014) Portaria MMA n. 443, de 17 de dezembro de 2014. Reconhece como espécies da flora brasileira ameaçadas de extinção aquelas constantes da lista nacional oficial de espécies da flora ameaçadas de extinção (Ordinance MMA no. 443, of december 17, 2014. Recognizes as species of Brazilian flora threatened with extinction those included in the official national list of species of flora threatened with extinction)
- Molinari AM, Simon R, Pfeiffer RM (2005) Prediction error estimation: a comparison of resampling methods. *Bioinformatics* 21(15):3301–3307. <https://doi.org/10.1093/bioinformatics/bti499>
- Muñiz GIB, Nisgoski S, Shardsosin FZ, França RF (2012) Anatomia do carvão de espécies florestais (Anatomy of forest species charcoal). *CERNE* 18(3):471–477. <https://doi.org/10.1590/s0104-7762012000300015>
- Muñiz GIB, Carneiro ME, Batista R, Rodrigues F, Zatt Shardsosin F, Nisgoski S (2016) Wood and charcoal identification of five species from the miscellaneous group known in Brazil as “angelim” by near-IR and wood anatomy. *Maderas Ciencia y tecnología* 18(3):505–522. <https://doi.org/10.4067/s0718-221x2016005000045>
- Nasirzadeh M, Khazael AA, bin Khalid M, (2010) Woods recognition system based on local binary pattern. 2010 2nd International Conference on Computational Intelligence. In: *Communication Systems and Networks*, IEEE, pp 308–313
- Ojala T, Pietikäinen M, Harwood D (1994) Performance evaluation of texture measures with classification based on kullback discrimination of distributions. In: *Proceedings of 12th International Conference on Pattern Recognition*, IEEE, vol 1, pp 582–585. <https://doi.org/10.1109/icpr.1994.576366>
- Ojala T, Pietikäinen M, Mäenpää T (2002) Multiresolution gray-scale and rotation invariant texture classification with local binary patterns. *IEEE Trans Pattern Anal Mach Intell* 24(7):971–987. <https://doi.org/10.1109/tpami.2002.1017623>
- Pace MR, Angyalossy V (2013) Wood anatomy and evolution: a case study in the bignoniaceae. *Int J Plant Sci* 174(7):1014–1048. <https://doi.org/10.1086/670258>
- Paula Filho PL, Oliveira LS, Nisgoski S, Britto AS (2014) Forest species recognition using macroscopic images. *Mach Vis Appl* 25(4):1019–1031. <https://doi.org/10.1007/s00138-014-0592-7>
- Pietikäinen M, Ojala T, Xu Z (2000) Rotation-invariant texture classification using feature distributions. *Pattern Recognit* 33(1):43–52. [https://doi.org/10.1016/s0031-3203\(99\)00032-1](https://doi.org/10.1016/s0031-3203(99)00032-1)
- Procópio LC, Secco RdS (2008) A importância da identificação botânica nos inventários florestais: o exemplo do “tauari” (Couratari spp. e Cariniana spp.-lecythidaceae) em duas áreas manejadas no estado do Pará (The importance of botanical identification in forest inventories: the example of “tauari” (Couratari spp. and Cariniana spp. - lecythidaceae) in two areas managed in the state of Pará). *Acta Amaz* 38:31–44. <https://doi.org/10.1590/S0044-59672008000100005>
- PROTA (2002) Protabase, Plant Resources of Tropical Africa/Ressources végétales de l’Afrique tropicale. Wageningen, Netherlands
- Quirk JT (1980) Wood anatomy of the vochysiaceae. *IAWA J* 1(4):172–179. <https://doi.org/10.1163/22941932-90000717>

- Ravindran P, Costa A, Soares R, Wiedenhoef AC (2018) Classification of CITES-listed and other neotropical meliaceae wood images using convolutional neural networks. *Plant Methods* 14(1). <https://doi.org/10.1186/s13007-018-0292-9>
- Refaeilzadeh P, Tang L, Liu H (2009) Cross validation, *Encyclopedia of Database Systems (EDBS)*. Arizona State University, Springer, New York, pp 532–538
- Richter H, Dallwitz M (2009) Commercial timbers: descriptions, illustrations, identification, and information retrieval. version: 25th june 2009
- Siew KF, Tang XJ, Tay YH (2017) Improved convolutional networks in forest species identification task. In: Jiang X, Arai M, Chen G (eds) *Second International Workshop on Pattern Recognition, SPIE*, <https://doi.org/10.1117/12.2280616>
- Soffiatti P, Boeger MRT, Nisgoski S, Kauai F (2016) Wood anatomical traits of the araucaria forest, southern Brazil. *Bosque* 37(1):21–31. <https://doi.org/10.4067/s0717-92002016000100003>
- Tortorelli LA (1956) *Maderas y bosques argentinos (Argentine woods and forests)*. Editorial Acme, Buenos Aires
- Venables WN, Ripley BD (2002) *Modern Applied Statistics with S*, 4th edn. Springer, New York
- Wheeler EA, Baas P, Gasson PE et al (1989) Iawa list of microscopic features for hardwood identification. *IAWA Bulletin* 10(3):
- White L, Gasson P (2008) *Mahogany*. Kew Publishing, Royal Botanic Gardens
- Yadav AR, Anand R, Dewal M, Gupta S (2015) Multiresolution local binary pattern variants based texture feature extraction techniques for efficient classification of microscopic images of hardwood species. *Appl Soft Comput* 32:101–112. <https://doi.org/10.1016/j.asoc.2015.03.039>
- Yigit E, Sabanci K, Toktas A, Kayabasi A (2019) A study on visual features of leaves in plant identification using artificial intelligence techniques. *Comput Electron Agric* 156:369–377. <https://doi.org/10.1016/j.compag.2018.11.036>
- Yusof R, Khalid M, Khairuddin ASM (2013) Application of kernel-genetic algorithm as nonlinear feature selection in tropical wood species recognition system. *Comput Electron Agric* 93:68–77. <https://doi.org/10.1016/j.compag.2013.01.007>

Publisher's Note Springer Nature remains neutral with regard to jurisdictional claims in published maps and institutional affiliations.